PAN
ARCHIVES OF ACOUSTICS
Vol. **44**, No. 3, pp. 533–541 (2019)
DOI: 10.24425/aoa.2019.129268

Improving Sound Transmission Through Triple-Panel Structure Using Porous Material and Sonic Crystal

Myong-Jin KIM

Department of Physics, Kim Il Sung University
Pyongyang, Democratic People's Republic of Korea; e-mail: mj_kim7093@163.com

(*received November 20, 2018; accepted May 15, 2019*)

Main aim of this study is to combine the characteristics of the sonic crystal (SC) with acoustic panels and porous materials to improve the sound transmission loss (STL) through the triple-panel structure. SCs cause a bandgap centered around a certain frequency (Bragg's frequency) due to generation of destructive interference. Initially, an analytical method is developed that extends the previous theory of double-panel structure to predict STL through a triple-panel structure. Finite element (FE) simulations are performed to obtain the STL through the triple-panel, which are validated with the analytical predictions. Various configurations are analyzed using the FE method based on the method of inserting the porous material and SCs between the panels to address the combined effect. STL through the triple-panel structure is compared with that through the double-panel structure having the same total weight and total thickness. It is found that the combined structure of the triple panel and the SC with glass wool as filler gives the best soundproof performance for the same external dimensions. For narrow air gaps, filing with glass wool is more advantageous than inserting one row of SC. In addition, the triple panel combined with a SC has better soundproofing than the two-panel counterparts.

Keywords: sound transmission loss; sonic crystal; triple-panel structure; sound insulation.

1. Introduction

Acoustic panels are widely used for sound insulation purposes in a variety of engineering application. The double-wall structure provides superior performance over a wide frequency range. Xin *et al.* (2008) conducted an analytical and experimental study of STL in a double-panel structure with an enclosed air cavity. Doutres and Atalla (2010) conducted an analytical study of a double-panel with multilayer absorbing blankets. Pellicier and Trompette (2007) studied various methods of calculating the sound reduction index, and the numerical results agree well with the experimental results. Arjunan *et al.* (2014) performed a three-dimensional vibration-acoustic FE modelling to calculate the sound reduction index of a stud-based double panel. Putra *et al.* (2013) conducted an experimental study of a microperforated panel (MPP) inserted between a double leaf partition. Wang *et al.* (2005) performed theoretical modelling of the effect of vertical metal studs placed between two panels on STL. Kang and Bolton (1996) did a theoretical study of a double panel lined with foams. Bolton *et al.* (1996) presented a theoretical modelling of sound transmission through laterally infinite double-panel structured lined with poroelastic materials in a diffuse field. Panneton and Atalla (1996), and Sgard *et al.* (2000) calculated the normal and random incidence STLs through finite double panels lined with porous materials, respectively, using FE method and boundary element (BE) method. Lee *et al.* (2007) used a topology optimization for sound transmission through normal incidence multilayered foams. However, their assumption that difference between boned and unbonded multilayers is insignificant is contradictory to the finding by Bolton *et al.* (1996) and Zhou *et al.* (2013a; 2013b). Tanneau *et al.* (2006) employed a genetic algorithm to optimize multilayered panels with a combination of solid, fluid and porous components.

A triple-panel structure has better mechanical, thermal and sound insulation properties than its double-panel counterpart, so it can replace the double-panel structures in soundproofing. Triple-glazing windows or triple-leaf walls without absorbent lining exhibit poor sound insulation performance in the low fre-

quency range compared to its double-leaf counterparts with the same total weight and total air gap depth (Bies, Hansen, 2009). Experiments by Tadeu and Mateus (2001) showed that the triple glazing exhibited reasonable improvements compared to the double glazing yet with the penalty in weight and volume. Xin and Lu (2011) presented an analytical model for sound transmission of clamp-mounted triple-panel partitions, but this model does not take into account the effect of poroelastic lining. Sharp (1973) suggested an empirical model for predicting the STL of a triple-panel wall with at least 2 in of fiberglass batts in each cavity. Measurements by Quirt (1983) showed that STL for a triple-glazing window below the fundamental resonance frequency is slightly larger than a double-glazing window as predicted by Brekke (1981). Liu (2015) extended Bolton *et al.* model (1996) for predicting STLs of double-panel structures lined with poroelastic materials to deal with the problems of triple-panel structures on the basis of Biot's theory (1956) and transfer matrix method showed the obvious advantages of the triple-panel structure with poroelastic materials.

SCs are composed of periodical solid scatter arrays embedded in a host material, which was first observed in 1995 in nature (Martinez-Sala *et al.*, 1995). Later on, it was also found that periodical scatterer arrays show good sound attenuation (Sanchez-Perez *et al.*, 2002). Due to the occurrence of destructive interference, sound waves with wavelengths equal to half the periodic constant cannot propagate in the SC (Gupta *et al.*, 2011). Sanchez-Dehesa *et al.* (2011) studied a SC combined with the recycled material (absorbing rubber crumb or porous material) and showed that the porous material in perforated scatterers increases the soundproof performance of a SC and that three rows of cylinders are enough to get well defined bandgaps. Gulia and Gupta (2018a) presented a compounded single-column model of SC and showed that the first bandgap of single-column SC appears in the lower frequency range than the multi-column SC with the same area and the same filling factor. Garcia-Raffi *et al.* (2018) showed a significant amount of broadband noise attenuation by using a SC made of rigid scatterers in water. Guild *et al.* (2018) designed a sound absorber using a SC made of a functionally graded material and showed the presence of zero transmittance over a given frequency region. Gulia and Gupta (2018b) inserted a SC and porous material in the double panel to study their individual and combined effect. Results showed that the combined structure of the double panel and the SC with glass wool filling gives the best STL for all cases for the same external dimensions.

In this present work, STL through the triple-panel structure with air gap is calculated by means of reflection and transmission coefficients using analytical method and compared with FE simulation results. In addition, SCs and porous materials are inserted between the panels to study their individual and combined effects. Further, STL of a triple-panel structure with the SC is compared with a double-panel counterpart to explorer its potential advantages.

2. Theoretical formulation

An analytical method is presented to calculate STL through the triple-panel by means of the reflection and transmission coefficients. z_1, z_2, z_3, z_4, z_5, z_6, and z_7 in Fig. 1a are the acoustic impedance of media A_1, A_2, A_3, A_4, A_5, A_6, and A_7, respectively and l_1, l_2, l_3, l_4, l_5, and l_6 are the width of media. A_1, A_3, A_5, and A_7 are air domains while A_2, A_4, and A_6 are panel domains. p is the sound pressure, u denotes the particle velocity. p_{1i}, p_{1r}, and p_{1t} are sound pressures of incidence, reflected, and transmitted wave, respectively. Subscripts and represent transmitted and reflected wave, respectively. The travelling wave components in each domain can be expressed as

$$\begin{aligned}
p_{1i} &= A_i e^{i(\omega t - k_1 x)}, & p_{1r} &= A_r e^{i(\omega t + k_1 x)},\\
p_{2t} &= B_i e^{i(\omega t - k_2 x)}, & p_{2r} &= B_r e^{i(\omega t + k_2 x)},\\
p_{3t} &= C_i e^{i(\omega t - k_3 x)}, & p_{3r} &= C_r e^{i(\omega t + k_3 x)},\\
p_{4t} &= D_i e^{i(\omega t - k_4 x)}, & p_{4r} &= D_r e^{i(\omega t + k_4 x)},\\
p_{5t} &= E_i e^{i(\omega t - k_5 x)}, & p_{5r} &= E_r e^{i(\omega t + k_5 x)},\\
p_{6t} &= F_i e^{i(\omega t - k_6 x)}, & p_{6r} &= F_r e^{i(\omega t + k_6 x)},\\
p_t &= G_i e^{i(\omega t - k_7 x)},
\end{aligned}$$

where A_i, A_r, B_i, B_r, C_i, C_r, D_i, D_r, E_i, E_r, F_i, F_r, and G_i are the complex sound pressure amplitudes, ω – the angular frequency, t – the time variable, x – the space variable, k_1, k_2, k_3, k_4, k_5, k_6, and k_7 are the wave vectors in media A_1, A_2, A_3, A_4, A_5, A_6, and A_7. As the interface considered is massless, both pressure and particle velocity at the interface should be continuous (Kinsler *et al.*, 2000)

$$|p_{1i} + p_{ir}|_{x=l_1} = |p_{2t} + p_{2r}|_{x=0}, \tag{1}$$

$$|u_{1i} + u_{ir}|_{x=l_1} = |u_{2t} + u_{2r}|_{x=0} \quad \Rightarrow$$

$$\left|\frac{A_i e^{i(\omega t - k_1 x)}}{z_1} - \frac{A_r e^{i(\omega t + k_1 x)}}{z_1}\right|_{x=l_1} = \left|\frac{B_i e^{i(\omega t - k_2 x)}}{z_2} - \frac{B_r e^{i(\omega t + k_2 x)}}{z_2}\right|_{x=0}. \tag{2}$$

Applying the boundary conditions at each interface (interface 1, 2, 3, 4, 5, and 6) and combining all the equations, the net reflection coefficient (R), which is the ratio of sound pressure level of reflected wave to the incident wave, is written as

$$R = e^{-2ik_1 l_1}\left\{\frac{(z_2 - z_1) + (z_2 + z_1)M}{(z_2 + z_1) + (z_2 - z_1)M}\right\}, \tag{3}$$

where

$$M = e^{-2ik_2l_2}\left\{\frac{(z_3-z_2)+(z_3+z_2)N}{(z_3+z_2)+(z_3-z_2)N}\right\},$$

$$N = e^{-2ik_3l_3}\left\{\frac{(z_4-z_3)+(z_4+z_3)P}{(z_4+z_3)+(z_4-z_3)P}\right\},$$

$$P = e^{-2ik_4l_4}\left\{\frac{(z_5-z_4)+(z_5+z_4)Q}{(z_5+z_4)+(z_5-z_4)Q}\right\},$$

$$Q = e^{-2ik_5l_5}\left\{\frac{(z_6-z_5)+(z_6+z_5)S}{(z_6+z_5)+(z_6-z_5)S}\right\},$$

$$S = e^{-2ik_6l_6}\frac{(z_7-z_6)}{(z_7+z_6)}.$$

The intensity transmission coefficient (T_I) is calculated using the formula (Kinsler *et al.*, 2000)

$$T_I = 1 - |R|^2. \tag{4}$$

3. FE analysis

There are three panels located at a certain distance as in Fig. 1. Aluminum sheets are used for the three panels. The thickness of the first and third panel is 0.8 mm while the second panel is 0.4 mm. The density of aluminum is 2700 kg/m^3, Young's modulus 70 GPa and Poison's ratio 0.33. The density of air

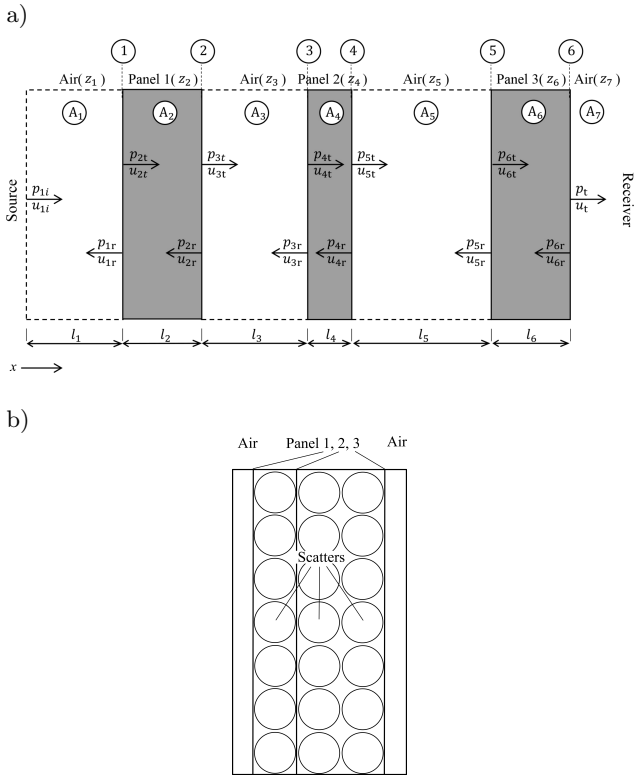

Fig. 1. Schematic of the triple-panel with two air gaps (a) and with three rows of scatters (b).

is ρ_0 = 1.25 kg/m^3 and the speed of sound in air is c = 343 m/s. A source of a plane wave is applied on the inlet of the triple-panel structure. Infinite radiation conditions are applied at the source and the receiver boundary. It can be assumed that there is no back reflection of the sound wave at the source and receiver boundary where following boundary conditions must be satisfied (Gulia, Gupta, 2018b)

$$\left(-\frac{\nabla p}{\rho}\right)\cdot n = \frac{i\omega}{\rho c_c}p - \frac{i\omega}{\rho c_c}p_0, \tag{5}$$

$$\left(-\frac{\nabla p}{\rho}\right)\cdot n = \frac{i\omega}{\rho c_c}p, \tag{6}$$

where $p = p_0e^{ikr}$, p is sound pressure, k – wave vector, r – direction vector, ρ – density, n – normal vector, ω – the angular frequency of the sound wave, and c_c – the sound speed. The remaining sides of the triple-panel structure are assumed to be rigid wall boundary. Particle velocity of sound wave perpendicular to the rigid wall boundary is zero. Neumann boundary condition is

$$\left(-\frac{\nabla p}{\rho}\right)\cdot n = 0. \tag{7}$$

To explor the effect of a SC on the soundproof performance of a triple-panel structure, the scatterers are inserted between the triple panel as in Fig. 1b. A number of cylindrical scatterers are arranged periodically inside the air cavity. Exterior surface of the scatterers is assumed to be sound hard. Repeat fully reflection on the scatterer's surface causes the destructive interference which leads to the formation of bandgaps in the SC.

Porous materials are widely used as a sound absorber for many practical applications. Models of the acoustics of porous materials include an empirical model (Delany, Bazley, 1970), analytical models (Allard, Atalla, 2009; Zwikker, Kosten, 1949), semi-phenomenological models (Johnson *et al.*, 1987; Champoux, Allard, 1991; Lafarge *et al.*, 1997) and Biot's model (1956). In this work, glass wool is taken as a porous material and the Delany-Bazley model is used to model the glass wool. Wave number (k_g) and characteristic impedance (z_g) of the glass wool are represented in the form of complex number as

$$k_g = k_a\left[1+0.098\left(\frac{\rho_a f}{R_g}\right)^{-0.7} - 0.189i\left(\frac{\rho_a f}{R_g}\right)^{-0.595}\right], \tag{8}$$

$$z_g = z_a\left[1+0.057\left(\frac{\rho_a f}{R_g}\right)^{0.734} - 0.087i\left(\frac{\rho_a f}{R_g}\right)^{-0.732}\right], \tag{9}$$

respectively, where $k_a = 2\pi f/c_a$, $z_a = \rho_a c_a$, ρ_a is density of air, c_a – sound speed in air, f – frequency, k_a – free space wave number, z_a – characteristic impedance of the air, and R_g is flow resistivity of glass wool. Mean

fiber diameter (d_g) and density (ρ_g) of glass wool are 10 μm and 12 kg/m^3, respectively. Flow resistivity can then be obtained as (Bies, Hansen, 1980)

$$R_g = \frac{3.18 \times 10^{-9} \rho_g^{1.53}}{d_g^2}. \tag{10}$$

Software ANSYS Multiphysics is used for FE calculation. For meshing, the maximum size of the element is taken as one eighth of the minimum wavelength (4 mm). STL is given by the ratio of sound power at receiver side to that at source side. Harmonic excitation is applied at the source and STL is calculated as the average sound power difference between the source and the receiver side.

4. Results and discussion

In this work, STL is calculated in the triple panels for different widths of two air cavity (parameter l_3, l_5 in Fig. 1) for a fixed total width ($l_2 + l_3 + l_4 + l_5 + l_6$ = 102 mm) and panel thickness ($l_2 = l_6$ = 0.8 mm, l_4 = 0.4 mm) using analytical method and FE simulation. Figure 2 shows the STL calculated using the analytical method versus FE simulation at 4 different widths of the air cavities. The width of the first air gap varies from 1cm to 4cm while the second varies from 9 cm to 6 cm. As shown in Fig. 2, the analytical results are in good agreement with the FE simulation results. Two kinds of resonances are observed in Fig. 2, i.e. the "mass-spring" resonance and the standing-wave resonance. The resonance frequencies of the equivalent "mass-air-mass-air-mass" system are as follows (Xin, Lu, 2011):

$$f_{m1,2} = \frac{\sqrt{2}}{4\pi} \sqrt{\frac{\lambda_1 + \lambda_2 \mp \sqrt{(\lambda_1 - \lambda_2)^2 + 4\kappa_1 \kappa_2 m_{s1}^2 m_{s3}^2}}{m_{s1} m_{s2} m_{s3}}}, \tag{11}$$

where $\lambda_1 = \kappa_1 m_{s3}(m_{s1} + m_{s2})$ and $\lambda_2 = \kappa_2 m_{s1}(m_{s2} + m_{s3})$ are the equivalent stiffnesses of the two air gaps

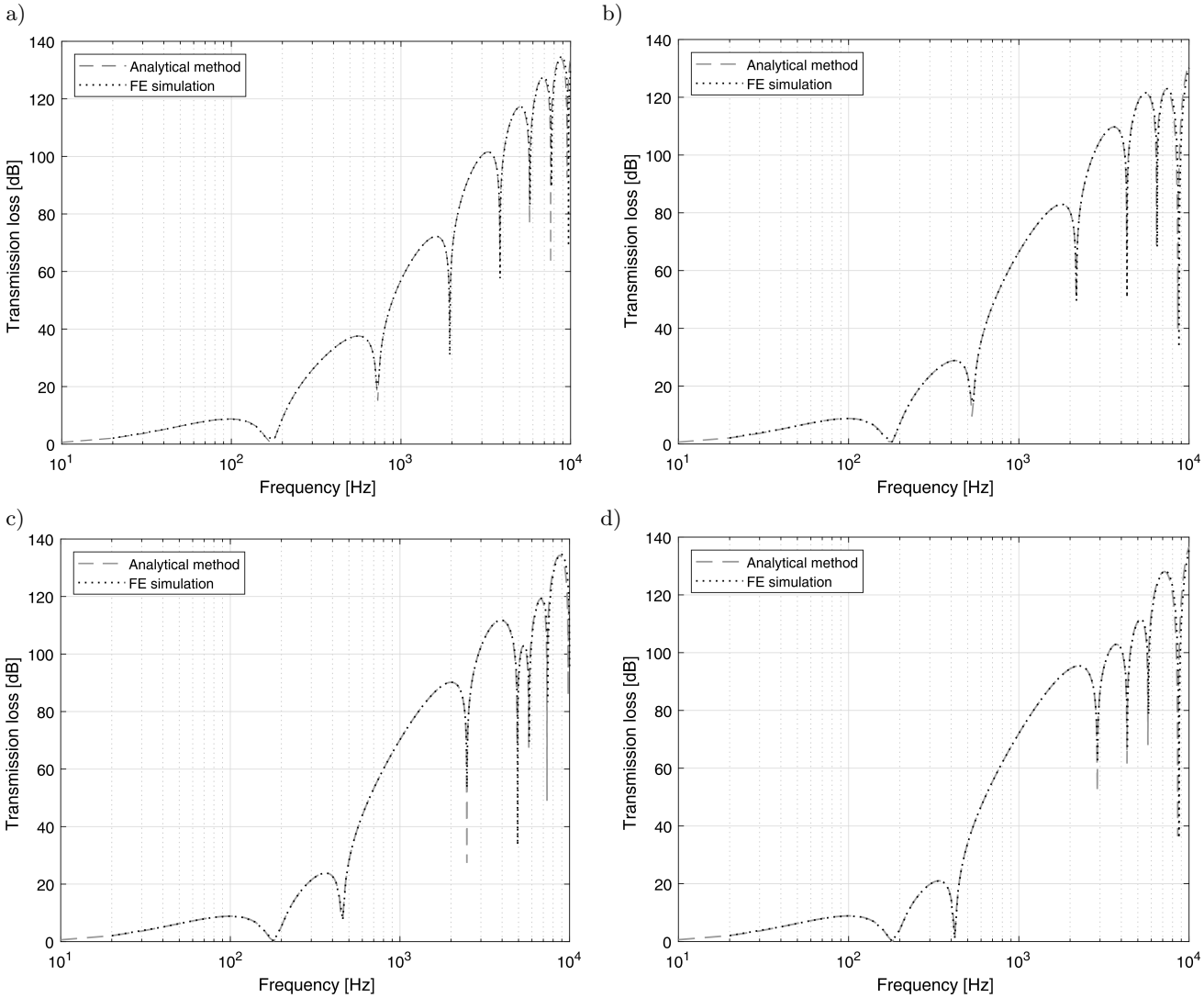

Fig. 2. STL through the triple panel calculated by the analytical method vs. FE simulation; air gaps are: a) 1 cm, 9 cm, b) 2 cm, 8 cm, c) 3 cm, 7 cm, d) 4 cm, 6 cm.

and $\kappa_{1,2} = \rho_0 c^2/l_{3,5}$, $m_{si}(i = 1,2,3)$ is the mass per unit area of three panels. When the widths of two air gaps are 1 cm and 9 cm, the mass-spring frequencies calculated from Eq. (11) are 174 Hz and 738 Hz which are reproduced in Fig. 2a. Such a reproduction of dips in STL can be observed in Figs 2b–d. The standing-wave resonance occurs when the width of air gap (δ) matches integer numbers of the half wavelength of the incident sound, and the n-th standing-wave resonance frequency can be expressed as (Wang *et al.*, 2005)

$$f_{s,n} = \frac{nc}{2\delta} \qquad (n = 1,2,3,\cdots). \tag{12}$$

Except for the first two dips in Figs 2a–d, the remaining dips represent the standing-wave resonance, which also match well with that calculated from Eq. (12).

To enhance the efficiency of double-panel structure, porous material and SCs are inserted inside the air gaps between panels. The scatterers are inserted between the air gaps of a triple panel as well as the porous material and the coupled effect of panel, porous material and a SC is investigated. Schematic diagram of the triple-panel structure is shown in Fig. 1b. The total width is $l_2+l_3+l_4+l_5+l_6 = 130.4$ mm and the thickness of panels are $l_2 = l_6 = 0.8$ mm, $l_4 = 0.4$ mm. The width of the first air gap (l_3) is 4.28 cm while the width of the second (l_5) is 8.56 cm. In the present work, glass wool is taken as a porous material and scatterers are cylindrical in shape. Radius of scatterers is 2 cm and lattice constant is 4.28 cm. Accordingly, one row of SC can be inserted into the first air gap and two rows of SC can be inserted into the second air gap. And panels are at a distance of half the lattice constant from the centre of the scatterers.

The STL calculated using FE simulation for various configuration of the triple-panel structure is shown in Fig. 3. Figure 3a shows STLs for four configurations with air filling between the second and the third panel, i.e. air-air, air-wool, air-SC and air-wool (SC).

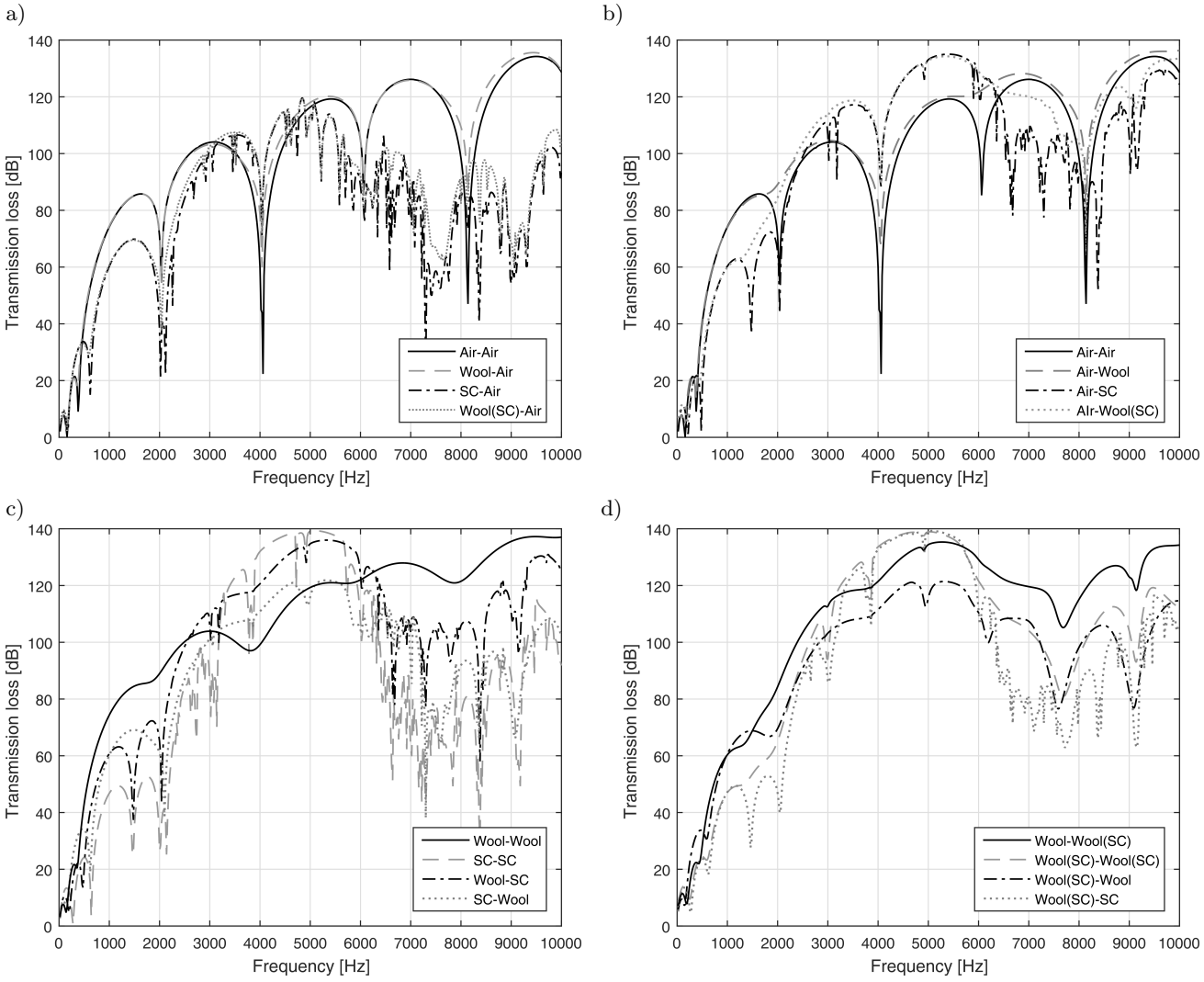

Fig. 3. STL in the triple-panel structure calculated by FE simulation: $l_2 + l_3 + l_4 + l_5 + l_6 = 130.4$ mm, $l_2 = l_6 = 0.8$ mm, $l_4 = 0.4$ mm, $l_3 = 4.28$ cm, $l_5 = 8.56$ cm: a) second gap filled with air, b) first gap filled with air, c) SCs not embedded in the glass wool, d) SCs embedded in the glass wool.

Figure 3b shows that with air filling between the first and the second panel. Figures 3c and 3d correspond to the cases for those with SCs embedded in the glass wool and not embedded. There are some sudden dips in STL through the panels with air gap which may be due to the "mass-spring" resonance and the "standing-wave" resonance as mentioned in Fig. 2. However, such a resonance is damped out by adding the glass wool. This leads to elimination of those sudden dips in the triple panel in all graphs.

Introducing a SC causes a bandgap due to destructive interference which results in improvement of STL in a particular range centered around Bragg's frequency. For the lattice constant of 4 cm, the Bragg's frequency is 4007 Hz, around which the broad bandgap is present in all graphs. Bragg's bandgap becomes higher and broader with increasing rows of scatterers. However, it can be observed in Fig. 3a that the effect of one row of SC on STL is not distinct, on the contrary, the sound insulation performance is less than the case with air gap in the high frequency range (above 5 kHz in this work). There are some unusual dips in STL through the SC-triple panel assembly, which might be associated with the complex interaction between the SC and the triple panel. The efficiency of a SC gets more distinct in Fig. 3b. In addition, when SC is embedded in the glass wool, the dips due to the resonances and the interaction between the SC and the panels can be eliminated which leads to enhancement of soundproof performance over the entire frequency range. It can be observed in Fig. 3c that insertion of one row of SC into the first air gap results in the worst sound insulation. And glass wool filling in the first gap and inserting SC and glass wool assembly in the second gap gives the best sound insulation. Such a tendency is also shown in Fig. 3d. If the first gap is filled with glass wool instead of one row of SC, the Bragg's bandgap becomes wider (solid line in Fig. 3d). It can therefore be concluded that triple panel-SC-glass wool assembly

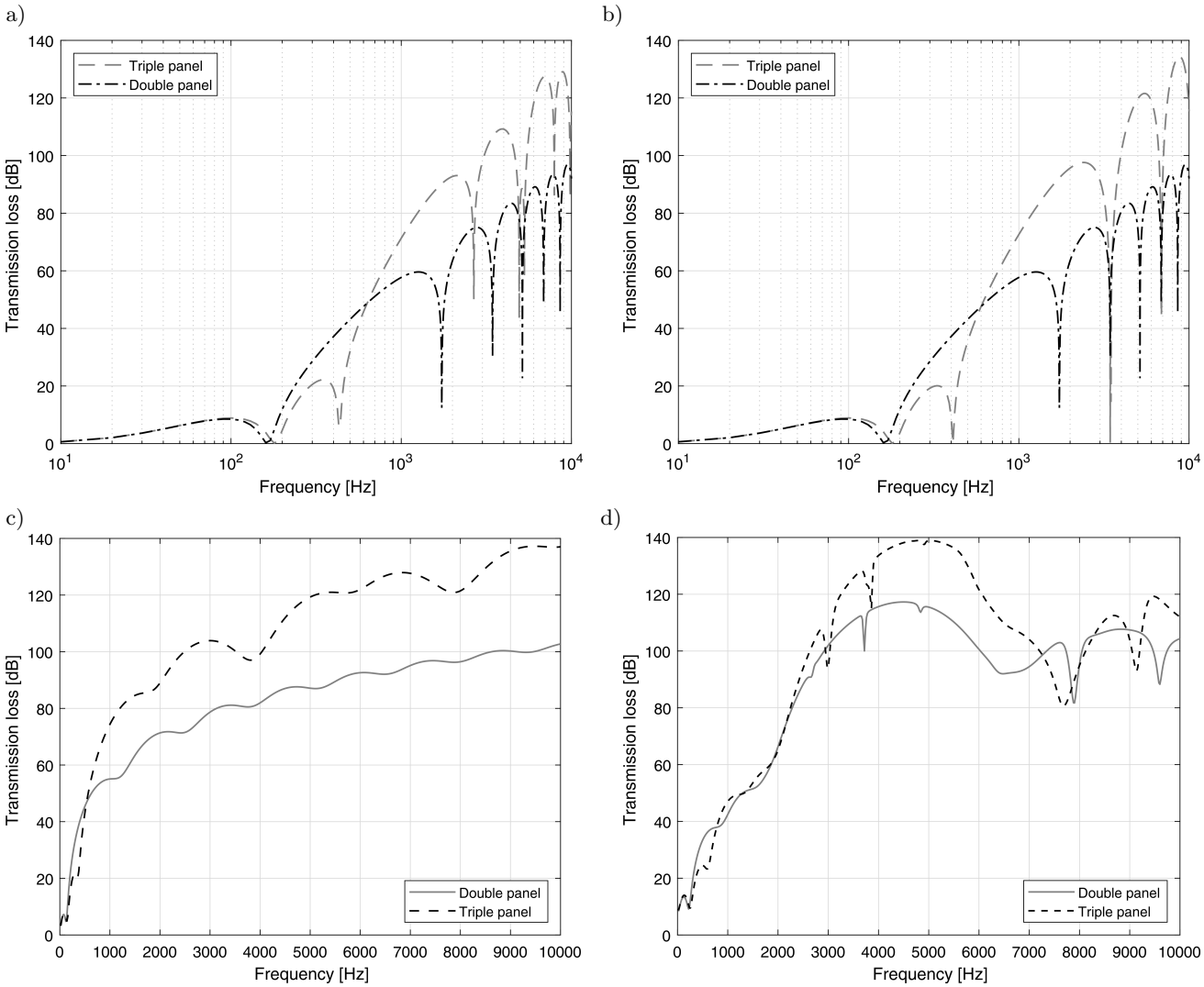

Fig. 4. Comparison of STL of a triple-panel structure and a double-panel counterpart: a) with two air gaps (3.5 cm, 6.5 cm), b) with two air gaps (5 cm, 5 cm), c) with glass wool in two gaps, d) with SCs embedded in glass wool.

gives the best STL for all cases for the same external dimensions. And the intensity of sound attenuation by one row of SC is very weak, it rather reduces the overall soundproofing performance of the triple-panel structure. This might be because the number of rows is one in the fundamental direction of sound propagation (normal to the panel), and complex interaction of sound waves occurs between the panels and scatterers. Therefore, if the air gap is narrow so as to insert only one row of SC, it is reasonable to fill it with glass wool.

Figure 4 shows STL through the triple-panel structure vs. that through the double-panel counterpart with the same total mass and total thickness. In order to equalize the mass, the plate thickness was set to 0.8 mm, 0.4 mm, and 0.8 mm for the triple-panel structure, and 1 mm and 1 mm for the double-panel structure. Figures 4a and 4b show the case where two gaps between the panels are filled with air. The width of the air gaps is $l_3 = 3.5$ cm, $l_5 = 6.5$ cm in Fig. 4a and $l_3 = l_5 = 5$ cm in Fig. 4b. From these figures, it can be seen that the STL of the triple panel is higher than the double panel by more than 20 dB on average in the middle and high frequency bands. Figure 4c shows the case where two gaps between the panels are filled with glass wool while Fig. 4d the case where three rows of scatterers are embedded in glass wool. Figure 4c shows that the STL of the triple-panel structure is 20 dB higher than the double-panel in the entire frequency region. It can also be seen from Fig. 4d that the triple-panel structure gives more than 20 dB higher peak of STL around the Bragg's frequency than that of the double-panel counterpart. Considering the fact that the sound insulation performance of wool-wool (SC) configuration (solid line in Fig. 3d) is higher than that of wool (SC)-wool (SC) configuration (dashed line in Fig. 3d), the triple-panel structure is possible to provide better soundproofing properties than the double-panel structure while reducing the overall weight.

5. Conclusions

In this paper, a previous work (Gulia, Gupta, 2018b) on improving the sound transmission loss through the double-panel structure using porous material and sonic crystal has been extended to address the problem of a triple-panel structure. First, we presented an analytical method for calculating the STL of a triple panel with two air gaps by means of the reflection and transmission coefficients. FE simulations were performed for several structures with different widths of air gap between panels and compared with analytical results, the two results agree very well. Next, we investigated the combined effect of panel, glass wool, and SC by using FE study on the various configurations where glass wool and SC are inserted in the air gaps. SCs cause a bandgap centered around Bragg's frequency, which results in a great enhancement of the soundproof performance. The Bragg's bandgap gets higher and wider with increasing rows of scatterers in SC. The porous material plays a role of eliminating the sudden dips of the STL caused by the "mass-spring" resonance and the "standing wave" resonance and the complex interaction between the SC and the panels in the triple-panel structure. The combined structure of panel, glass wool, and SC gives better soundproofing than all other cases. Meanwhile, if one row of SC is located in a narrow gap, the sound insulation characteristics gets much worse in the medium and high frequency bands. This suggests that the influence of SC on the sound attenuation, as shown in previous studies, is highly depended on the number of rows of scatterers. It also shows that it is more reasonable to insert perforated materials instead of one row of SC in a multi-panel structure with a gap narrow enough to accommodate one row. Finally, STL of a triple-panel structure was compared with a double-panel structure with same total mass per unit area and total thickness. The triple-panel structure filled with porous material exhibited 20 dB higher sound insulation characteristics than the double-panel counterpart in the entire frequency band. Also, even though the number of scatterers' row is smaller than double-panel structure, the triple-panel structure has higher STL in the entire frequency band. In other words, a triple-panel structure has potential to provide better soundproofing properties than the double-panel structure, reducing the overall weight.

Acknowledgments

I wish to thank the anonymous reviewers for their valuable comments, constructive remarks and suggestions to improve the quality of the paper.

References

1. Allard J.F., Atalla N. (2009), *Propagation of Sound in Porous Media:Modelling Sound Absorbing Materials*, John Wiley and Sons, Ltd., West Sussex.

2. Arjunan A., Wang C.J., Yahiaoui K. (2014), *Development of a 3D finite element acoustic model to predict the sound reduction index of stud based double-leaf walls*, Journal of Sound and Vibration, **333**, 6140–6155.

3. Bies D.A., Hansen C.H. (1980), *Flow resistance information for acoustical design*, Applied Acoustics, **13**, 357–391.

4. Bies D.A., Hansen C.H. (2009), *Engeneering Noise Control: Theory and Practice*, 4th edition, Spon Press, Abingdon, UK.

5. Biot M.A. (1956), *Theory of propagation of elastic waves in a fluid-saturated porous solid I. Low-*

frequency range. II. Higher frequency range, Journal of the Acoustical Society of America, **28**, 168–191.

6. Bolton J.S., Shiau N.M., Kang Y.J. (1996), *Sound transmission through multi-panel structures lined with elastic porous materials*, Journal of Sound and Vibration, **191**, 317–347.

7. Brekke A. (1981), *Calculation methods for the transmission loss of single, double and triple partitions*, Applied Acoustics, **14**, 225–240.

8. Champoux Y., Allard J. (1991), *Dynamic tortuosity and bulk modulus in air-saturated porous media*, Journal of Applied Physics, **70**, 4, 1975–1979.

9. Delany M.E., Bazley E.N. (1970), *Acoustical properties of fibrous absorbent materials*, Applied Acoustics, **3**, 105–116.

10. Doutres O., Atalla N. (2010), *Acoustic contributions of a sound absorbing blanket placed in a double panel structure: Absorption versus transmission*, Journal of the Acoustical Society of America, **128**, 664–671.

11. Garcia-Raffi L.M., Salmeron-Contreras L.J., Herrero-Dura I. (2018), *Broadband reduction of the specular reflections by using sonic crystals: A proof of concept for noise mitigation in aerospace applications*, Aerospace Science and Technology, **73**, 300–308.

12. Guild M.D., Rothk M., Sieck C.F., Rohde C., Gregory O. (2018), *3D printed sound absorbers using functionally-graded sonic crystals*, Journal of the Acoustical Society of America, **143**, 1714–1714.

13. Gulia P., Gupta A. (2018a), *Increasing low frequency sound attenuation using compounded single layer of sonic crystal*, AIP Conference Proceedings, 1953, pp. 140072:1–4, India.

14. Gulia P., Gupta A. (2018b), *Enhancing the sound transmission loss through acoustic double panel using sonic crystal and porous material*, Journal of the Acoustical Society of America, **144**, 1435–1442.

15. Gupta A., Lim K.M., Chew C.H. (2011), *Analysis of frequency band structure in one-dimensional sonic crystal using Webster horn equation*, Applied Physics Letters, **98**, 201906.

16. Johnson D.L., Koplik J., Dashen R. (1987), *Theory of dynamic permeability and tortuosity in fluid-saturated porous media*, Journal of Fluid Mechanics, **176**, 379–402.

17. Kang Y.J., Bolton J.S. (1996), *A finite element model for sound transmission through foam lined double panel structure*, Journal of the Acoustical Society of America, **99**, 2755–2755.

18. Kinsler L.E., Frey A.R., Coppens A.B., Sanders J.V. (2000), *Fundamentals of Acoustics*, Wiley, California.

19. Lafarge D., Lemarinier P., Allard J.F. (1997), *Dynamic compressibility of air in porous structures at audible frequencies*, Journal of the Acoustical Society of America, **102**, 1995–2006.

20. Lee J.S., Kim E.I., Kim Y.Y., Kim J.S., Kang Y.J. (2007), *Optimal poroelastic layer sequencing for sound transmission loss maximization by topology optimization method*, Journal of the Acoustical Society of America, **122**, 2097–2106.

21. Liu Y. (2015), *Sound transmission through triple-panel structures lined with poroelastic materials*, Journal of Sound and Vibration, **339**, 376–395.

22. Martinez-Sala R., Sancho J., Sanchez J.V., Gomez V., Llinares J., Meseguer F. (1995), *Sound attenuation by sculpture*, Nature, **378**, 6554, 241–241.

23. Panneton R., Atalla N. (1996), *Numerical prediction of sound transmission through finite multilayer systems with poroelastic materials*, Journal of the Acoustical Society of America, **100**, 346–354.

24. Pellicier A., Trompette N. (2007), *A review of analytical methods, based on the wave approach to compute partitions transmission loss*, Applied Acoustics, **68**, 1192–1212.

25. Putra A., Ismail A.Y., Ramlan R., Ayob R., Py M.S. (2013), *Normal incidence of sound transmission loss of a double-leaf partition inserted with a microperforated panel*, Advances in Acoustics and Vibration, 216493.

26. Quirt J.D. (1983), *Sound transmission through windows II. double and triple glazing*, Journal of the Acoustical Society of America, **74**, 534–542.

27. Sanchez-Dehesa J., Garcia-Chocano V.M., Torrent D., Cervera F., Cabrera S., Simon F. (2011), *Noise control by sonic crystal barriers made of recycled materials*, Journal of the Acoustical Society of America, **129**, 1173–1173.

28. Sanchez-Perez J.V., Rubio C., Martinez-Sala R., Sanchez-Grandia R., Gomez V. (2002), *Acoustic barriers based on periodic arrays of scatterers*, Applied Physics Letters, **81**, 27, 5240–5242.

29. Sgard F.C., Atalla N., Nicolas J. (2000), *A numerical model for the low frequency diffuse field sound transmission loss of double-wall sound barriers with elastic porous linings*, Journal of the Acoustical Society of America, **108**, 2865–2872.

30. Sharp B.H. (1973), *A Study of Techniques to Increase of the Sound Insulation of Building Elements*, PB 222 829, U.S. Department of Commerce, National Technical Information Service (NTIS).

31. Tadeu A.J.B., Mateus D.M.R. (2001), *Sound transmission through single, double and triple glazing. Experimental evaluation*, Applied Acoustics, **62**, 307–325.

32. Tanneau O., Casimir J.B., Lamary P. (2006), *Optimization of multilayered panels with poroelastic compo-*

nents for an acoustical transmission objective, Journal of the Acoustical Society of America, **120**, 1227–1238.

33. Wang J., Lu T.J., Woodhouse J., Langley R.S., Evans J. (2005), *Sound transmission through lightweight double-leaf partitions: Theoretical modelling*, Journal of Sound and Vibration, **286**, 817–847.

34. Xin F.X., Lu T.J. (2011), *Analytical modeling of sound transmission through clamped triple-panel partition separated by enclosed air cavities*, European Journal of Mechanics A/Solids, **30**, 770–782.

35. Xin F.X., Lu T.J., Chen C.Q. (2008), *Vibroacoustic behavior of clamp mounted double-panel partition with enclosure air cavity*, Journal of the Acoustical Society of America, **124**, 3604–3612.

36. Zhou J., Bhaskar A., Zhang X. (2013a), *Optimization for sound transmission through a double-wall panel*, Applied Acoustics, **74**, 1422–1428.

37. Zhou J., Bhaskar A., Zhang X. (2013b), *Sound transmission through a double-panel construction lined with poroelastic material in the presence of mean flow*, Journal of Sound and Vibration, **332**, 3724–3734.

38. Zwikker C., Kosten C.W. (1949), *Sound Absorbing Materials*, Elsevier, New York.